The Journal of Neuroscience, March 1987, 7(3): 742–752

Acetylcholine Causes Rapid Nicotinic Excitation in the Medial Habenular Nucleus of Guinea Pig, *in vitro*

David A. McCormick and David A. Prince

Department of Neurology, Stanford University School of Medicine, Stanford, California 94305

The actions of ACh in the medial habenular nucleus (MHb) were investigated using extra- and intracellular recording techniques in guinea pig thalamic slice maintained *in vitro*. Applications of ACh to MHb neurons resulted in rapid excitation followed by inhibition. Neither of these responses was abolished by blockade of synaptic transmission, indicating that they are consequences of ACh action directly on MHb cells. Local applications of the nicotinic agonists nicotine and cytisine caused long-lasting excitation, while applications of another nicotinic agonist, 1,1-dimethyl-4-phenylpiperazinium caused both the excitatory and inhibitory responses. Applications of the muscarinic agonists DL-muscarine and acetyl-β-methylcholine did not consistently cause either the excitatory or inhibitory response. Adding the nicotinic antagonist hexamethonium to the bathing medium blocked both the excitatory and inhibitory ACh responses, while addition of the muscarinic antagonists atropine or scopolamine had no effect. These results indicate that the effects of ACh on MHb neurons are mediated by nicotinic receptors.

Intracellular recordings revealed that ACh or nicotine cause an increase in membrane conductance associated with depolarizations that had an average reversal potential of −16 to −11 mV. These results indicate that the ACh-induced excitation is due to an increase in membrane cation conductance.

The inhibitory response that follows ACh-induced depolarization and repetitive firing was associated with a hyperpolarization and an increase in membrane conductance. Similar postexcitatory inhibition could also be elicited by direct depolarization or by applications of glutamate, indicating that the hyperpolarizing response to ACh may be an endogenous postexcitatory potential that is not directly coupled to activation of nicotinic receptors. These results suggest that cholinergic transmission in the MHb may be largely of the nicotinic type. This nucleus may be of one of the major regions of the nervous system through which nicotine mediates its central effects.

Received Apr. 25, 1986; revised Aug. 25, 1986; accepted Aug. 26, 1986.

We thank Dr. B. W. Connors for comments on the manuscript, J. Kadis for technical assistance, and Walter Carlini for help with the potassium-sensitive microelectrodes. This study was supported by NIH Grants NS 12151 and NS 06477 (D.A.P.) and NS 07331 (D.A.M.) from the National Institute of Neurological Communicative Diseases and Stroke, by the Morris Research Fund, and by fellowships from the Huntington's Disease Foundation of America and the Giannini Foundation (D.A.M.).

Correspondence should be addressed to David A. McCormick, Ph.D., Department of Neurology, Rm. C338, Stanford University Medical Center, Stanford, CA 94305.

The medial habenular nucleus (MHb) is a collection of closely spaced cells on the dorsal–medial surface of the thalamus. This nucleus receives its major input via the stria medularis from the postcommissural septum (Gottesfeld and Jacobowitz, 1979; Herkenham and Nauta, 1979; Contestabile and Fonnum, 1983) and gives rise to a large axonal projection through the fasciculus retroflexus to the interpeduncular nucleus at the base of the brain (Herkenham and Nauta, 1979). Both the afferents and efferents of the MHb have been proposed to be at least in part cholinergic (Kataoka et al., 1973, 1977; Kuhar et al., 1975; Gottesfeld and Jacobowitz, 1979; Vincent et al., 1980; Contestabile and Fonnum, 1983; Houser et al., 1983; Villani et al., 1983; Keller et al., 1984; Woolf and Butcher, 1986). Recent immunohistochemical studies for choline acetyltransferase (ChAt), the synthesizing enzyme for ACh, show that the ventral portions of the MHb as well as many fibers in the fasciculus retroflexus are heavily reactive (Houser et al., 1983). Lesions of the septal region, stria medularis, MHb, or fasciculus retroflexus reduce ChAt activity in both the medial habenular and interpeduncular nuclei (Kataoka et al., 1973, 1977; Gottesfeld and Jacobowitz, 1978, 1979; Vincent et al., 1980; Contestabile and Fonnum, 1983; Contestabile and Villani, 1983). These results imply that the MHb may receive a cholinergic projection from the diagonal band/posterior septal region, while the interpeduncular nucleus may receive a cholinergic input from this region as well as from the medial habenular nuclei (however, see Woolf and Butcher, 1985).

Autoradiographic localization of putative cholinergic receptors shows that the MHb contain a high density of nicotinic, but not muscarinic, receptors (Rotter et al., 1979; Martin and Aceto, 1981; Clarke et al., 1984, 1985; Rainbow et al., 1984; London et al., 1985). Furthermore, recent autoradiographic labeling of the presumed α-subunit of neural nicotinic receptors shows that the MHb is heavily reactive (Boulter et al., 1986; Goldman et al., 1986). These results indicate that cholinergic transmission in the MHb may be largely nicotinic.

Intracellular studies of the postsynaptic actions of ACh in the CNS have been almost exclusively limited to those involving muscarinic receptors (see references in Krnjević, 1975, and McCormick and Prince, 1986a, b). Traditional nicotinic receptor-mediated excitation, similar to that seen in the Renshaw cells of the spinal cord (Curtis and Ryall, 1966), has been observed in only a limited number of nuclei, including the interpeduncular nucleus (Brown et al., 1983; Takagi, 1984) and perhaps some nuclei of the brain stem (Bradley and Dray, 1972), hypothalamus (Cobbett et al., 1986), and thalamus (Phillis, 1971).

In this study, we describe a rapid nicotinic excitatory response to ACh in the MHb that appears to be due to an increase in membrane cation conductance.

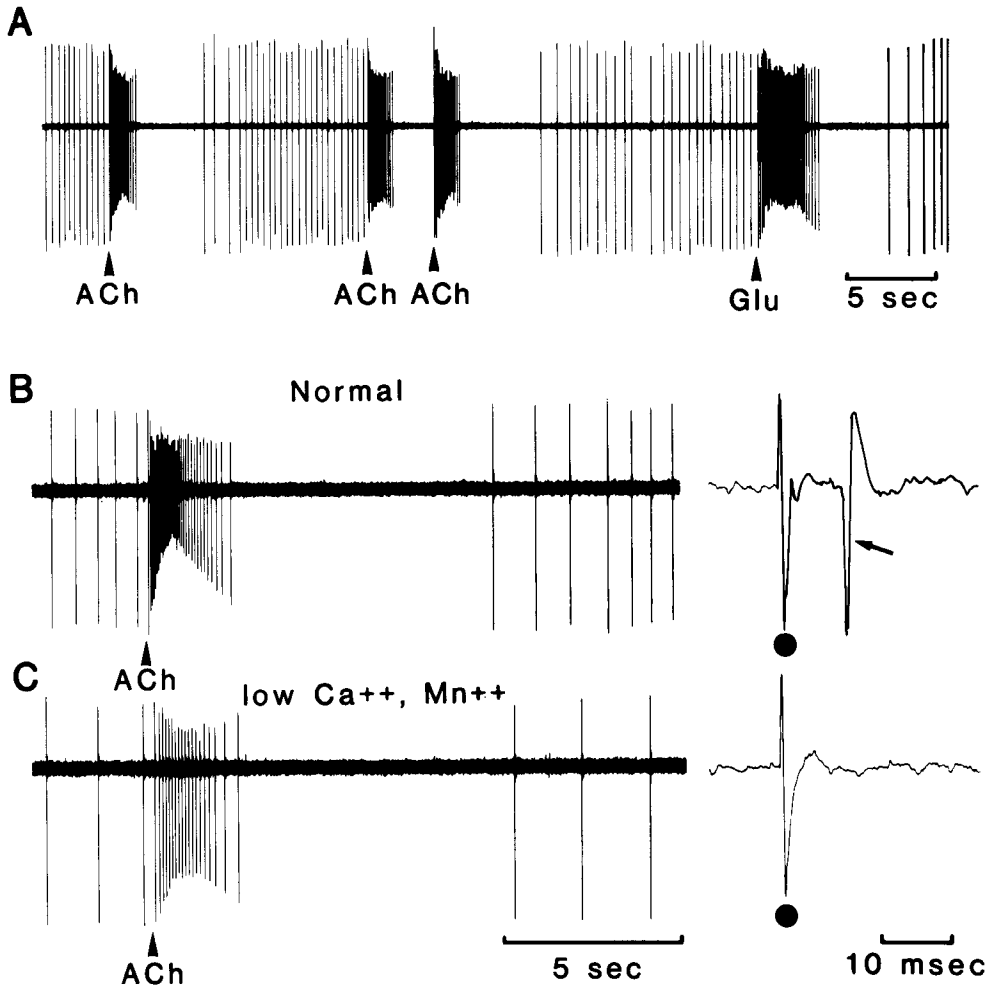

Figure 1. Extracellular recordings of responses to ACh. *A,* Application of ACh causes a rapid excitation followed by inhibition. A second application of ACh during the inhibitory period results in an additional excitatory–inhibitory sequence, indicating that the inhibition is not a result of depolarization block. Application of glutamate to this neuron also causes excitation followed by inhibition. *B,* Application of ACh to this MHb neuron in normal solution causes the typical excitation–inhibition sequence. Stimulation in the region of the stria medularis fiber pathway (*filled circle*) consistently activates an action potential (*B*: *right, arrow*). *C,* After approximately 30 min in Mn^{2+} (5 mM) and 0 Ca^{2+} containing solution, the neuron still responds to ACh with an excitation and inhibition, although the spontaneous firing rate in this neuron has decreased. Stimulation of synaptic inputs (*C, right*) does not activate action potentials, indicating that synaptic transmission is blocked. The ACh-induced excitatory response is reduced in Mn^{2+}, low CA^{2+}, perhaps due to hyperpolarization of the neuron, as indicated by the reduced spontaneous firing rate, or some change in spike threshold during 5 mM Mn^{2+} perfusion. Calibrations under first and second segments of *C* are also for comparable segments of *B*.

Materials and Methods

Procedures for preparing thalamic slices and obtaining intracellular recordings from them have been described previously (Jahnsen and Llinás, 1984; McCormick and Prince, 1986b). Male or female adult guinea pigs were anesthetized with sodium pentobarbital (30 mg/kg) and decapitated. A block of thalamus and cortex containing the MHb was rapidly removed, placed in cold (5°C) slice solution, and cut into 400–500 μM slices on a vibratome (Lancer Corporation). Slices were maintained in an interface type recording chamber at a temperature of 36 ± 1°C. The control bathing medium contained the following (in mM): NaCl, 124; KCl, 2.5 or 5; $MgSO_4$, 2; NaH_2PO_4, 1.25; $NaHCO_3$, 26; $CaCl_2$, 2; and dextrose, 10. When divalent cations (e.g., Mn^{2+}) were added, PO_4 and SO_4 were omitted to prevent precipitation and the solution contained the following: NaCl, 132; KCl, 5; $MgCl_2$, 2; $NaHCO_3$, 22; and dextrose, 10. The slice solution was saturated with 95% O_2/5% CO_2 and buffered to pH 7.4.

All agonists were applied using the pressure pulse technique. Brief pulses of pressure [approximately 40 psi (280 KPa), 10 msec] were used to extrude approximately 0.1–5 pl of agonist-containing slice solution from a broken micropipette. Repeated applications of ACh at different depths in the slice were used to find a region from which robust responses were obtained. In experiments in which acetyl-β-methylcholine (MCh) was to be applied, the site of best response to ACh was first determined and a second microelectrode containing MCh was lowered to approximately the same point in the slice. To further insure an adequate application of MCh, the volume of application was increased to 10–15 pl at a concentration of 5 mM. Nicotine, cytisine, and 1,1-dimethyl-4-phenylpiperazinium (DMPP) were applied only to the surface of the slice since this was found to be sufficient to cause large responses. Antagonists were applied in the bathing medium. All drugs were obtained from Sigma. The MHb could be readily identified in the thalamic slice under the dissecting microscope. It lay on the most dorsomedial aspect of the thalamus, just dorsal and medial to the end of the fasciculus retroflexus.

Intracellular recordings were obtained with microelectrodes fabricated on a Brown and Flaming P-80/PC puller and beveled to a final resistance of 150–175 MΩ. Bridge balance was continuously monitored. Only neurons with steady resting membrane potentials of at least −50 mV and overshooting action potentials were included in the intracellular study. Extracellular recordings were obtained with broken intracellular microelectrodes filled with the bathing medium. These microelectrodes had a resistance of 10–25 MΩ. All data were recorded on tape (0–5 KHz for intracellular recordings; 300–5 KHz for extracellular units) and a strip-chart recorder. In some experiments, extracellular [K] was measured using valinomycin K^+-sensitive microelectrodes (Oehme and Simon, 1976) connected to an axoprobe-1 amplifier (Axon Instruments). These K^+-sensitive microelectrodes registered no response when placed in the ACh-containing application solution, indicating that our $[K]_o$ measurements were not contaminated by applications of this agent.

Results

Extracellular single-unit recordings indicated that the neurons of the MHb are spontaneously active in the slice, firing in a regular, repetitive manner at approximately 2–6 Hz (Fig. 1). Application of ACh (0.5–1.0 mM) to MHb neurons resulted in a short-latency excitation followed by a period of inhibition of spike discharge (Fig. 1*A*). Similar responses were obtained from

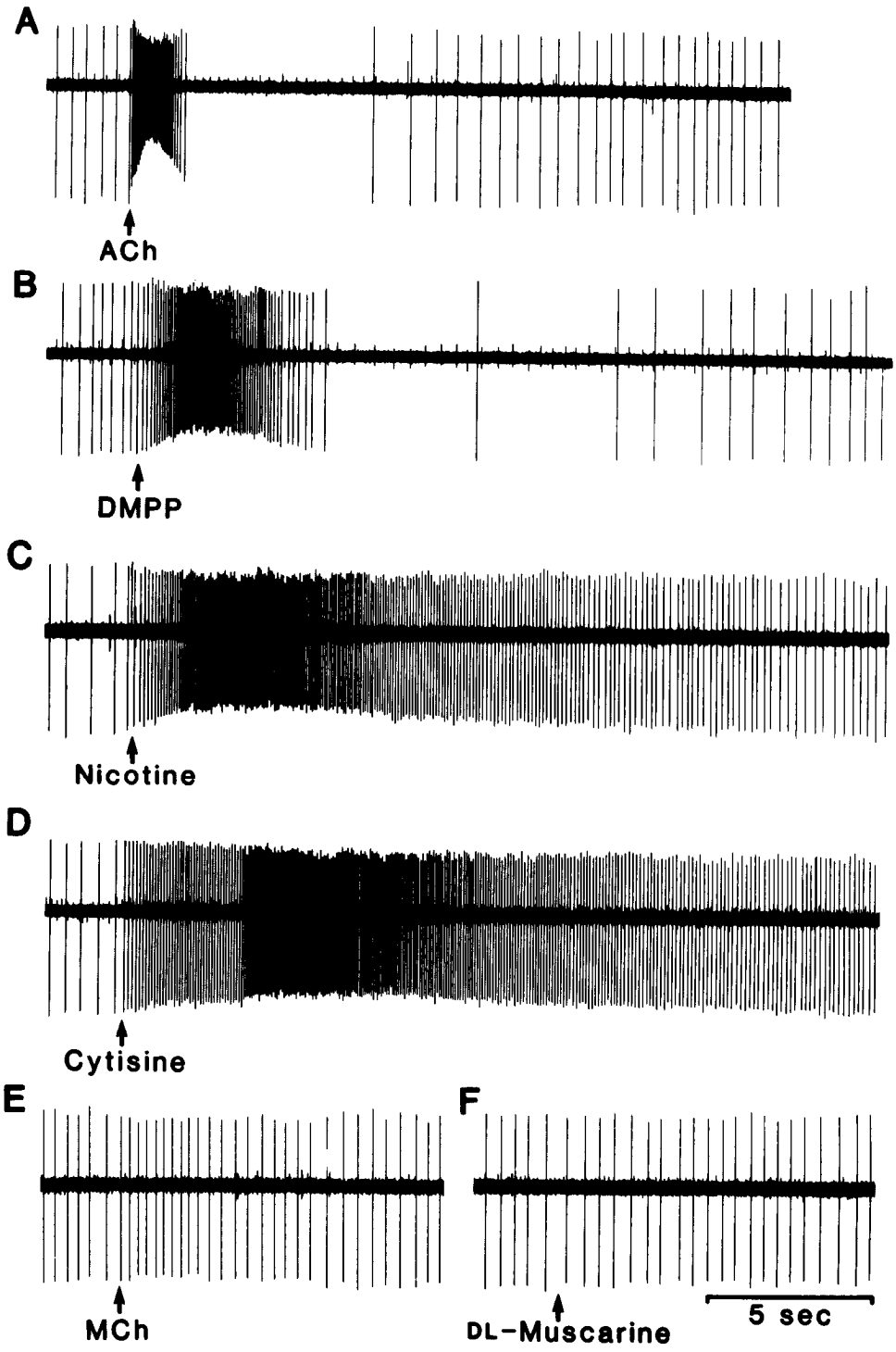

Figure 2. Pharmacological characterization of receptors mediating responses to ACh in the MHb. *A,* Application of ACh to this neuron causes the typical excitation–inhibition sequence. *B,* Application of the nicotinic agonist DMPP also causes excitation followed by inhibition. *C* and *D,* In contrast, application of the nicotinic agonists nicotine and cytisine causes prolonged excitation with little or no inhibition. Application of the muscarinic agonist acetyl-β-methylcholine (*MCh*) causes only a weak excitation (*E*), while DL-muscarine causes no response (*F*). All data in *A–F* are from the same MHb neuron.

neurons at all locations within the nucleus (e.g., ventral versus dorsal). The inhibitory response always occurred after the initial excitation and was never seen in isolation. The duration and intensity of both the excitation and inhibition became greater with increasing doses of ACh. Applications of the excitatory amino acid glutamate (Glu, 1 mM) resulted in a similar excitatory–inhibitory response (Fig. 1*A*). The excitatory responses to ACh and Glu were often associated with a transient decrease in action potential amplitude and an increase in action potential width. The action potential amplitude could even be transiently eliminated, indicating that depolarization block may have occurred (for example, see Fig. 3*A*, normal and wash—arrow). However, the action potentials usually began to recover before the period of inhibition, indicating that the late period of spike inhibition was not merely the result of depolarization block (Brown, 1980). This conclusion was supported by the finding that additional applications of ACh or of Glu during the late period of inhibition resulted in an additional excitatory–inhibitory sequence (Fig. 1*A*, second and third ACh applications). Interestingly, in many cells, the first few spikes after the period of inhibition had amplitudes that were generally larger than those of spikes before ACh application (e.g., Fig. 1, *A, B*). This may indicate that the membrane potential is hyperpolarized during the period of inhibition.

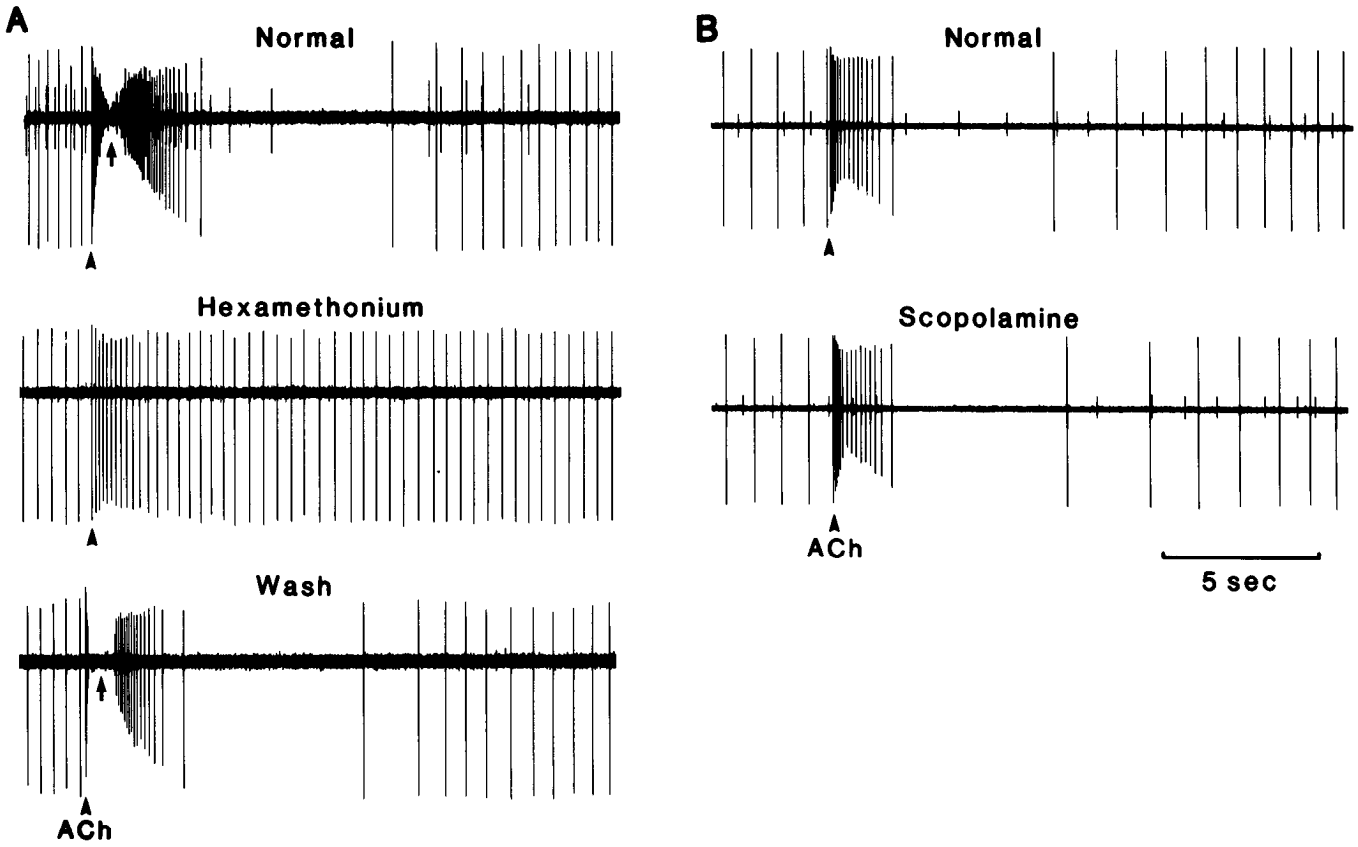

Figure 3. Effect of nicotinic and muscarinic antagonists on the response of MHb neurons to ACh. *A,* Application of ACh to this MHb neuron in normal solution results in the typical excitation–inhibition sequence. Washing in of the nicotinic antagonist hexamethonium (250 μM) greatly diminishes the excitatory and inhibitory responses. Washing out of the hexamethonium reinstates a strong excitation–inhibition response. The lack of action potentials during the midportion of the excitatory response (*arrow*) is probably due to depolarization block. The loss of a second, smaller-amplitude unit during the recording contributed to the change in appearance of the response to ACh in wash versus normal segments. *B,* Bath application of the muscarinic antagonist scopolamine (10 μM) for more than 45 min did not affect the excitatory or inhibitory response to ACh.

To test whether the excitatory–inhibitory responses to ACh were direct on the cells recorded or were mediated through the release of another neurotransmitter, sagittal thalamic slices were bathed in solutions containing Mn^{2+} (3–5 mM) and low Ca^{2+} (0.0—0.5 mM) to block synaptic transmission. Before block of synaptic transmission, both stimulation of the stria medularis fiber pathway (Fig. 1*B,* right) and application of ACh (Fig. 1*B,* left) caused short-latency excitatory responses of MHb neurons. The ACh-induced excitation was followed by the typical period of inhibition (Fig. 1*B*). After approximately 30 min of exposure to the Mn^{2+}, low Ca^{2+} solution, the synaptically evoked excitatory response was completely blocked, but the ACh-induced excitation and inhibition were not (n = 6; Fig. 1*C*). In fact, bathing the slices for more than 1 hr in 0.0 mM Ca^{2+}, 5 mM Mn^{2+} did not block either spontaneous activity or the excitatory and inhibitory ACh responses. These results indicate that both the excitatory and the inhibitory responses of MHb neurons to ACh are a consequence of direct action on the neuron studied and not mediated through the release of other neurotransmitters. Furthermore, the persistence of spontaneous activity in the nucleus following synaptic blockade indicates that this activity is intrinsic to MHb neurons and is not due to external synaptic drive.

Rapid excitatory responses to ACh have been associated with nicotinic as well as muscarinic receptors (Curtis and Ryall, 1966; Krnjević, 1975; Brown, 1980; Volle, 1980; Takagi, 1984; McCormick and Prince, 1985), while inhibitory responses are usually associated with receptors of the muscarinic type (e.g., see Krnjević, 1975; McCormick and Prince, 1986a). We investigated the pharmacological profile of the receptors mediating the responses of MHb neurons to ACh, using typical nicotinic and muscarinic agonists and antagonists. Local application of the nicotinic agonists nicotine (1 mM; n = 10) or cytisine (1 mM; n = 4) resulted in prolonged excitation, which was gradual in both its rise to peak firing frequency and decay back to baseline firing rates (Fig. 2, *C, D*). Inhibition was absent or only very weak. In contrast, application of the nicotinic agonist DMPP (Chen et al., 1951; see Table 2 in Gyermek, 1980) (1 mM; n = 7) caused excitation followed by prolonged inhibition (Fig. 2*B*). In general, the excitatory responses to DMPP were stronger and more rapid in onset and offset than responses to a similar application of nicotine or cytisine but not as rapid as responses to ACh. The ability of DMPP, but not nicotine, to generate the inhibitory response may be related to the prolonged action of nicotine due to its uptake and slow release by brain tissue (Brown et al., 1971).

In contrast to applications of nicotinic agonists, application of the muscarinic agonist MCh (5 mM; n = 9) (Curtis and Ryall, 1966) most often did not cause a response, though weak excitation or weak inhibition was occasionally seen with large doses

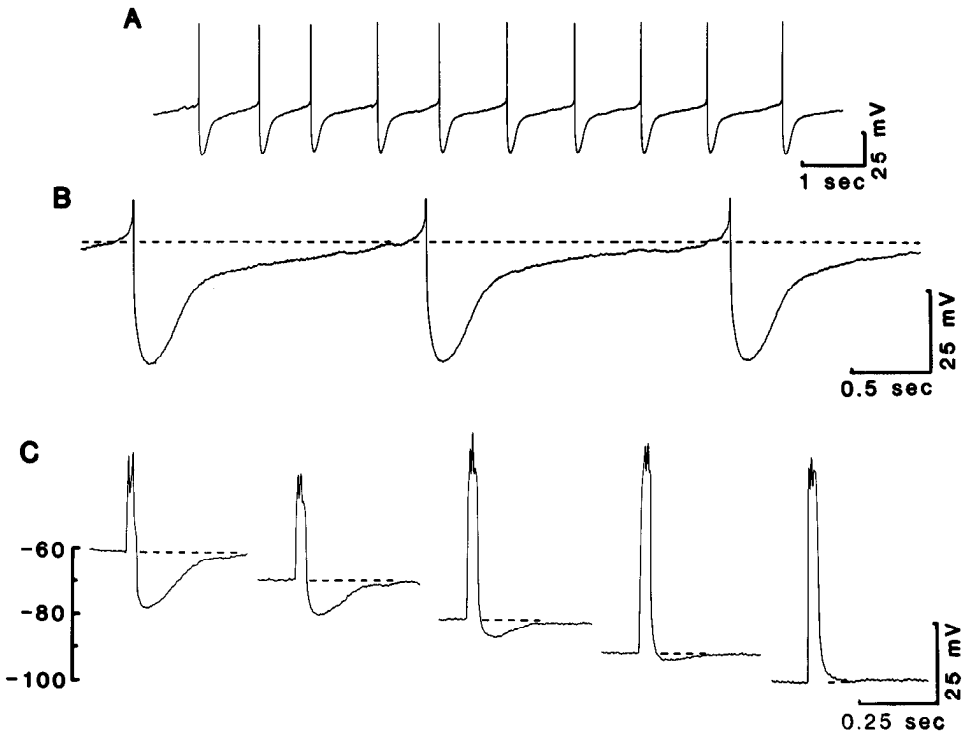

Figure 4. Characteristics of intracellularly recorded, spontaneously firing MHb neurons. *A*, Spontaneously occurring action potentials are followed by at least 2 phases of hyperpolarization. *B*, Segment of *A* expanded for detail. *Dashed line* drawn in at −55 mV. *C*, Reversal potential of the afterhyperpolarization (AHP). Activation of 2 action potentials by a short (30 msec) depolarizing pulse is followed by a substantial AHP that reverses polarity at about −95 mV (5 mM $[K]_o$). The amplitude of the injected current pulse was adjusted so as to cause the generation of 2 action potentials at each membrane potential. Action potential amplitudes are not fully shown.

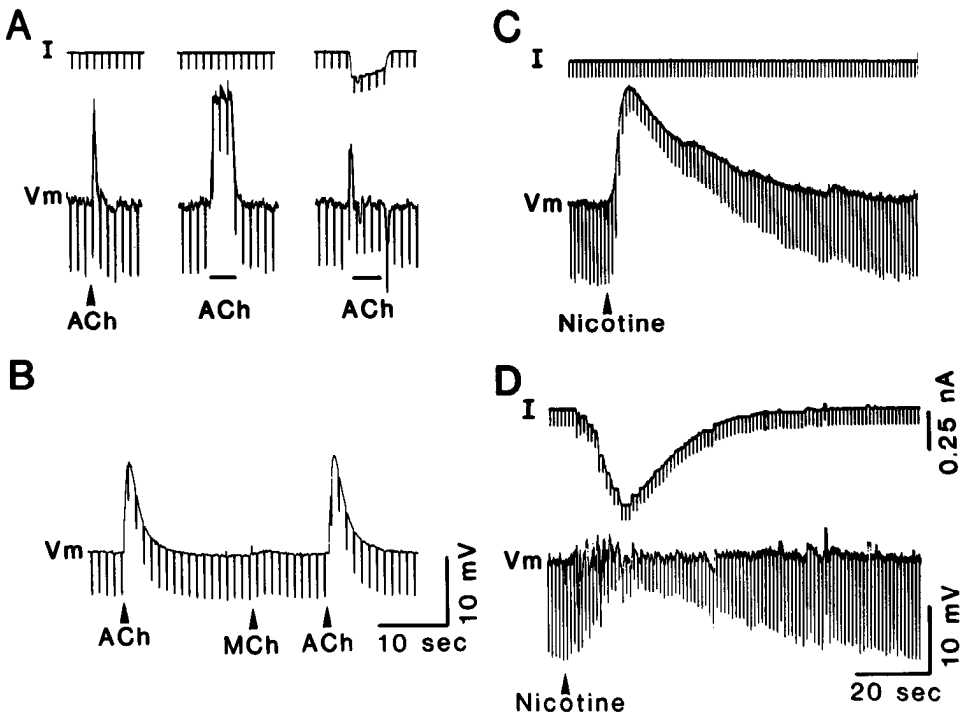

Figure 5. ACh causes short-latency nicotinic depolarization of MHb neurons. *A*, Application of a brief pulse of ACh to a MHb neuron causes a rapid depolarization (*A, left*). Lowering the pressure and prolonging the duration of application results in a more square-shaped response (*A, middle*). Adjusting the injected DC so as to compensate for the ACh-induced depolarization shows that ACh causes an increase in membrane conductance during the response associated with a peak inward current of approximately 170 pA (*A, right*). *Upper traces* are the current monitor, with hyperpolarizing current pulses being delivered at a rate of 1 Hz. *B*, Application of ACh to another MHb neuron causes typical depolarization, while application of the muscarinic agonist acetyl-β-methylcholine (*MCh*) evokes only a very small response. *C*, Application of a small amount of nicotine to the surface of the slice causes a large and prolonged depolarization. *D*, Manual voltage clamp so as to maintain a relatively constant membrane potential following nicotine application. Nicotine causes a large increase in membrane conductance, as indicated by a decrease in membrane electrotonic responses to hyperpolarizing current pulses. Current monitor shows that nicotine induces an inward current with a peak amplitude of about 660 pA. Calibration in *B* also for *A* and in *D* also for *C* and current trace of *A*.

(Fig. 2*E*). Similarly, applications of DL-muscarine (10 mM; n = 4) resulted in no response (Fig. 2*F*). These results indicate that the ACh-induced excitation and inhibition is the result of activation of nicotinic receptors. To confirm this hypothesis we added the specific nicotinic antagonist, hexamethonium (Paton and Zaimis, 1951; Brown, 1980), 100–500 μM, to the bathing medium (Fig. 3*A*). Hexamethonium reversibly antagonized both the excitatory and inhibitory responses to ACh (n = 5). Bath applications of the muscarinic antagonists scopolamine or atropine (10 μM), on the other hand, did not affect the ACh-induced excitation or inhibition (Fig. 3*B*; n = 4). These findings support the conclusion that ACh responses of MHb neurons are the result of the activation of nicotinic receptors.

Intracellular recordings

Intracellular recordings from MHb neurons in the ventral half of the nucleus indicated that these cells are remarkable for the presence of rather large input resistances of 50–500 MΩ ($\bar{X}$ = 144 ± 110 MΩ) and large afterhyperpolarizations (AHPs) (14–45 mV, 0.2 to >1 sec at firing threshold in 2.5 mM K), which followed even a single action potential (Fig. 4, *A, B*). Spontaneous activity was characterized by action potentials followed by AHPs that appeared to have both fast and slow components (Fig. 4, *A, B*). The large AHPs were associated with a substantial increase in membrane conductance and had a reversal potential of −88.1 mV (±3.3 mV; n = 6) in 5.0 mM extracellular K (Fig. 4*C*) and −106.7 mV (±3.9 mV; n = 4) in 2.5 mM K. This shift in equilibrium potential (62 mV per 10-fold change in $[K]_o$) indicates that the AHP is probably due to activation of a K current, as in other regions of the CNS (Hotson and Prince, 1980; Madison and Nicoll, 1984). MHb neurons completely lacked the low-threshold, voltage-sensitive, slow Ca^{2+} spike characteristic of other thalamic neurons (Jahnsen and Llinás, 1984; Wilcox et al., 1985).

To prevent the confounding factors associated with spontaneous neuronal discharge during applications of ACh, all cells were hyperpolarized with intracellular injection of DC before applications of agonists. After a few minutes of hyperpolarizing current injection, most MHb neurons spontaneously hyperpolarized to such an extent that resting potential remained below firing threshold after removal of the holding current, even though the same cells were originally spontaneously active upon initial stabilization of the membrane potential (e.g., Fig. 4). Under these circumstances, the average resting membrane potential was −63 mV (± 6.5 mV) and action potential amplitude was 76 mV (± 10.6 mV).

Brief (ca. 10 msec) pressure pulse applications of ACh to MHb neurons always resulted in a rapid depolarization with an onset latency that could be as brief as the delay imposed by the application system (i.e., approximately 10 msec) and a duration of approximately 0.5–5 seconds (Fig. 5, *A, B*). In most cells, these applications of ACh were kept small so as to avoid the generation of action potentials. Larger ACh applications, which generated action potentials, were associated with large membrane depolarizations followed by a hyperpolarization (see below). When long-duration (3–6 sec), low-pressure ACh pulses were applied, square-shaped depolarizations were evoked (Fig. 5*A*, second response). When intracellular injection of hyperpolarizing current was used to compensate for the ACh-induced depolarization, it was clear that ACh caused an increase in apparent membrane conductance (G_N), which ranged from 3 to >7 nS (Fig. 5*A*, third application). Much larger increases in G_N occurred with larger applications of ACh (e.g., see Fig. 7*A*).

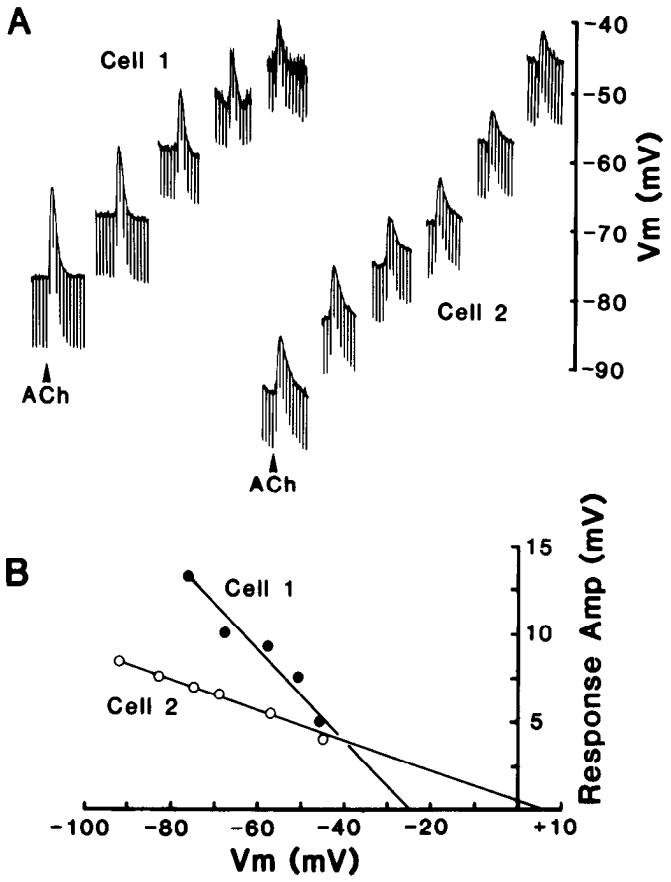

Figure 6. Estimation of the reversal potential of the rapid depolarizing response to ACh. *A*, Applications of ACh to 2 neurons at different membrane potentials (*scale at right*) indicate that the cholinergic depolarization becomes smaller at more positive V_m's. *B*, Plot of the data in *A* shows that the extrapolated reversal potentials for *Cells 1* and *2* are −25 and +5 mV, respectively. Reversal potentials for these 2 neurons represent 2 of the more extreme values for all neurons tested.

The nicotinic nature of this response was confirmed with intracellular recordings by applications of nicotine (Fig. 5, *C, D*) and MCh (Fig. 5*B*). Small applications of nicotine to the surface of the slice resulted in large depolarizations (Fig. 5*C*). When the injected current was adjusted during these responses so as to maintain a relatively constant V_m, it was apparent that nicotine caused a large increase in G_N of 5 to >10 nS (Fig. 5*D*). In contrast, applications of the muscarinic agonist MCh resulted in either no response or only very small depolarizations, whereas ACh caused the typical rapid excitatory response when applied to the same neurons (Fig. 5*B*).

Reversal potential of ACh-induced depolarization

The rapid excitatory response to ACh varied in amplitude when tested at various V_m's (Fig. 6). The response was largest at hyperpolarized V_m's, smallest at depolarized V_m's, and had extrapolated reversal potentials of −40 to +5 mV ($\bar{X}$ = −16.7 ± 18.1 mV; n = 5) (Fig. 6, *A, B*). In most MHb neurons, the input resistance appeared to be relatively constant over the range of V_m's tested (e.g., cell 2, Fig. 6*A*). However, in some neurons, R_N decreased substantially with depolarization (e.g., Cell 1, Fig. 6*A*). The possible effects of these nonlinearities in R_N upon the

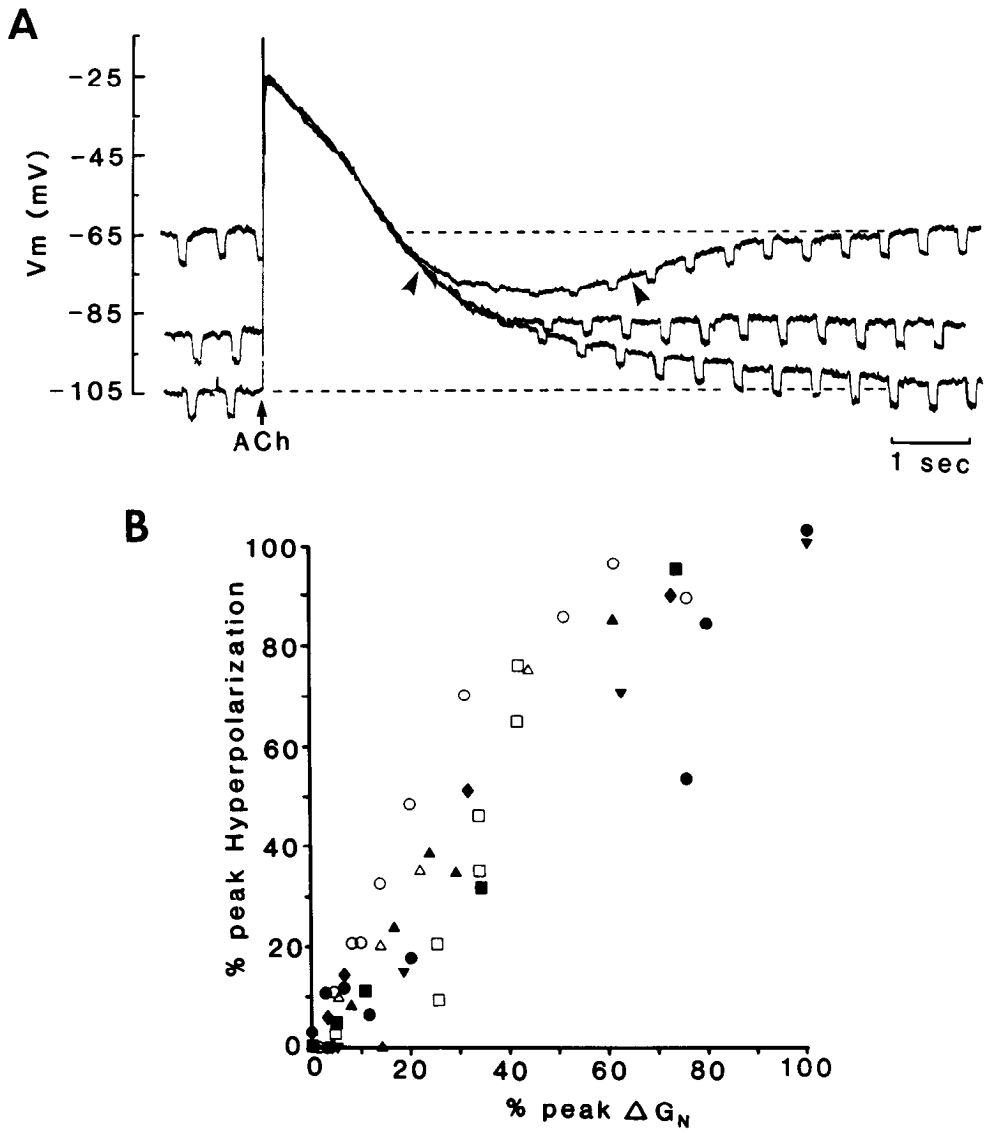

Figure 7. Characteristics of ACh-induced hyperpolarization. *A*, Large application of ACh to a MHb neuron held near firing threshold (−65 mV) causes a large depolarization and the generation of action potentials followed by a hyperpolarization. Both responses are associated with substantial increases in G_N. A second application of ACh at −90 mV results in a relatively steady membrane potential during the period of the hyperpolarizing response of the −65 mV application as G_N gradually returns to normal. Application of ACh with the cell hyperpolarized to −105 mV results in a slow depolarization during the inhibitory period, indicating that the hyperpolarization has been reversed. *B*, Plot of percentage peak hyperpolarization versus percentage peak change in G_N. Data were obtained from measurements at the peak of the hyperpolarization (100%) and as the membrane potential returned to normal for 8 cells that had first been depolarized to near firing threshold with intracellular injection of DC. Change in conductance (ΔG_N) was calculated as the input conductance during the hyperpolarization minus the input conductance at a comparable membrane potential after the response was over. The data are expressed as a percentage of the ΔG_N at the peak of the hyperpolarization. Note that the 2 measures are highly correlated (r = 0.92), and as the change in conductance declines to zero, so does the hyperpolarization. Different symbols represent different MHb neurons.

projected reversal potential were corrected by dividing the amplitude of the ACh response by R_N at each V_m tested. The projected reversal potential for ACh-induced depolarizations in MHb neurons after correction for nonlinearities in R_N was −14.7 mV (±18.5). Furthermore, given that the amplitude of the ACh response varied as a relatively linear function of V_m, it was also possible to calculate the extrapolated reversal potential of the ACh induced depolarization utilizing the manual voltage clamp technique and the following equation: $V_{reversal} = V_{clamp} + I_{clamp}/\Delta G_N$ (Ginsborg, 1967). Using this approach, the calculated reversal potential of the ACh-induced rapid excitation was −28 to +8 mV ($\bar{X}$ = −11.3 ± 13.5 mV; n = 4), in agreement with the above current-clamp results.

Postexcitatory hyperpolarization

Applications of ACh that generated large depolarizations and action potentials caused a postexcitatory hyperpolarization (n = 14; Fig. 7*A*; −65 mV application). When MHb neurons were allowed to be spontaneously active, application of ACh resulted in a rapid depolarization associated with the generation of action potentials, followed by a hyperpolarization during which the spontaneous spike activity ceased. The duration of this postexcitatory hyperpolarization ($\bar{X}$ = 7.4 ± 4.0 sec; n = 14) was similar to that of the inhibition seen in the extracellular recordings (e.g., see Figs. 1–3). The similarity in duration and the ability of the hyperpolarization to inhibit ongoing spike activity indicated that this response underlies the postexcitatory inhibitory phase seen with ACh applications during extracellular recordings (see Fig. 1). Therefore, we refer to this period of hyperpolarization as "ACh-induced inhibition or hyperpolarization" while making no assumptions as to whether this effect is direct (e.g., direct coupling of ACh receptors to K^+ channels) or indirect (e.g., caused by the previous generation of action potentials).

A comparison of the amplitude of V_m changes evoked by current test pulses during the ACh-induced hyperpolarization, versus those at similar V_m's after the response was over, revealed that the agonist-induced hyperpolarization was associated with an increase in membrane conductance of 3–45 nS ($\bar{X}$ = 16.8 ± 12.4 nS) at its peak. When ACh was applied with the neuron held at various V_m's, the evoked hyperpolarization became smaller at more negative values and could be reversed to a slow depolarization (Fig. 7*A*). The reversal potential of the ACh-induced hyperpolarization varied depending upon whether the

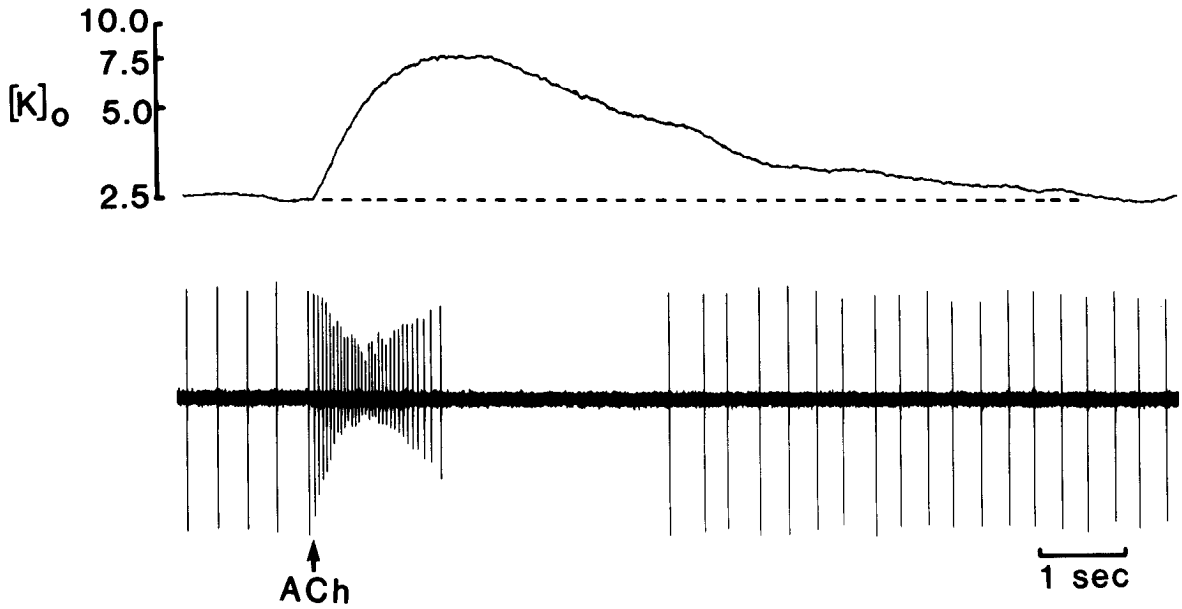

Figure 8. Simultaneous recording of $[K]_o$ measured with a valinomycin K^+-sensitive microelectrode and response of MHb neurons to application of ACh. ACh causes the typical excitation–inhibition sequence. During the excitation, $[K]_o$ is seen to increase to approximately 8 mM. This increase in $[K]_o$ gradually returns to normal, $[K]_o$ being in the range of 4–7.5 mM during the period of inhibition of spike activity. The $[K]_o$ of the bathing medium was 2.5 mM.

early or late components of the response were measured. The early portions (Fig. 7*A*, first arrow) reversed at a much more positive membrane potential than the later components (Fig. 7*A*, second arrow). These results indicate that the ACh-induced depolarization and hyperpolarization interact substantially during at least the early phases of the inhibitory response. However, it was usually possible to find a membrane potential at which the later components of the hyperpolarization were at a stable equilibrium potential as G_N increased back to normal (Fig. 7*A*, −90 mV application). This equilibrium potential varied from −75 to −90 mV in 2.5 mM K-containing bathing medium.

The presence of an increase in membrane conductance and a demonstrable reversal potential would seem to indicate that the hyperpolarizing response is due to an increase in membrane conductance to one or more ions, as opposed to activation of an electrogenic ionic pump (Brown et al., 1972; Nicoll and Alger, 1981; Thompson and Prince, 1986). However, similar results could be obtained if there were substantial overlap between an ACh-induced excitation and a strong electrogenic ionic pump. In this situation the apparent increase in membrane conductance during the hyperpolarization could be caused by the residual increase in cation conductance to ACh, while the apparent reversal potential would represent the V_m at which the depolarizing influence of the cation conductance is at equilibrium with the hyperpolarizing influence of the electrogenic ionic pump. To obtain some indication of whether the increase in membrane conductance was related to the generation of the hyperpolarization or merely reflected the residual influence of ACh upon cation channels, we plotted the relative amplitude of the change in neuronal input conductance (calculated as the difference in G_N during the ACh response and that at a similar V_m after the response was over) versus the relative amplitude of the hyperpolarizing phase (Fig. 7*B*). Such plots revealed that these 2 measures of the response parallel each other quite well, although in a somewhat curvilinear manner (Fig 7*B*). This nonlinearity may be due to a number of factors, including changes in the driving voltage between V_m and the reversal potential during different parts of the response, decay of a possible residual influence of the previous depolarization, or $[K]_o$ changes. The Pearson's correlation coefficient for these data ranged from 0.90 to 0.99 for individual cells and 0.92 ($p < 0.001$, $df = 49$) for all cells normalized to the same peak response (Fig. 7*B*) even in the presence of this nonlinear relationship. This result is most readily explained if the hyperpolarization is caused by an increase in membrane conductance to K or Cl, as opposed to activation of an electrogenic ionic pump.

The range at which the ACh-induced hyperpolarization reversed (−75 to −90 mV) is significantly positive to expected E_K (−106.7) in 2.5 mM $[K]_o$ (as measured from the reversal potential of the spike AHP). However, given the close apposition of MHb neurons to one another, often without intervening glial processes (Tokunaga and Otani, 1978), and the apparent increase in cation conductance during the ACh-induced depolarization, a substantial increase in extracellular [K] might be expected, thereby altering E_K. We tested this possibility by performing simultaneous extracellular [K] measurements with valinomycin K^+-sensitive microelectrodes and single-unit recordings with a second independent microelectrode during applications of ACh (Fig. 8). ACh caused an increase in $[K]_o$ up to peak levels of 15 mM from a baseline level of 2.5 mM during the period of excitation. This increase in $[K]_o$ gradually returned to normal over the course of many seconds (Fig. 8), with $[K]_o$ often being in the range of 5–8 mM during the period of inhibition (Fig. 8). Given an $[K]_o$ of 5–8 mM, a reversal potential of −75 to −90 mV is exactly as expected for increases in membrane K conductance (see above and McCormick and Prince, 1986a), indicating that the ACh-induced inhibition could be entirely due to an increase in gK.

Discussion

The results of the present study indicate that MHb neurons possess nicotinic receptors that, when activated, cause a rapid

excitation through an increase in membrane conductance. The average extrapolated reversal potential of this response (−11 to −16 mV) agrees well with that for ACh nicotinic responses in the PNS and neuromuscular junction, where ACh is known to cause an increase in membrane conductance to cations (Takeuchi and Takeuchi, 1960; Dennis et al., 1971; Gallagher et al., 1982). These results suggest that the ACh-induced rapid excitation in the MHb is also mediated by an increase in membrane conductance to cations. The presence of strong nicotinic responses and the apparent lack of muscarinic components following ACh applications to the MHb is consistent with autoradiographic findings that show that this nucleus has a high density of nicotinic, but not muscarinic, receptors (Rotter et al., 1979; Martin and Aceto, 1981; Clarke et al., 1984, 1985; Rainbow et al., 1984; London et al., 1985). The block of ACh responses by hexamethonium indicates that the nicotinic receptor in the MHb may be of the ganglionic (versus neuromuscular) type (Brown, 1980; Goldman et al., 1986).

A cholinergic synaptic input to the MHb has not yet been proven. It has been proposed that the MHb receives a cholinergic input from the postcommissural septal region (Kataoka et al., 1977; Gottesfeld and Jacobowitz, 1979; Contestabile and Fonnum, 1983). Recent double-labeling experiments (retrograde fluorescent dyes and ChAt immunoreactivity or AChE staining) indicate that the habenular nuclei may also recieve a cholinergic input from the horizontal limb of the diagonal band, magnocellular preoptic area, and the pedunculopontine and dorsolateral tegmental nuclei of the brain stem (Woolf and Butcher, 1986). However, the latter study did not determine which of the habenular nuclei (medial versus lateral) were the recipients of this presumed cholinergic innervation. Other anatomical studies confirm the presence of a projection to the MHb from the horizontal limb of the diagonal band (Domesick, 1976; Herkenham and Nauta, 1977). Much of the evidence for a cholinergic input to the MHb is based upon the loss of ChAt activity in the MHb after lesions of the septal region or stria medularis fiber pathway. Since some MHb neurons themselves appear to possess intrinsic ChAt activity (Houser et al., 1983; Keller et al., 1984), it is possible that these lesion-induced reductions in ChAt levels are transynaptic and not due to the loss of cholinergic terminals per se. Given the possible cholinergic nature of MHb neurons, an additional possible source of cholinergic input is recurrent collaterals within the nucleus itself (Iwahori, 1977). Confirmation of a cholinergic pathway to the MHb must await combined ChAt immunocytochemistry and electron microscopy. Our data do indicate that activation of such an input would almost certainly cause rapid nicotinic excitation. If this excitation were of sufficient amplitude, a postexcitatory period of inhibition would be expected, as reported here.

A number of different mechanisms may underlie the ACh-induced inhibition including: (1) direct coupling of nicotinic receptors to inhibitory mechanisms; (2) an indirect response due to an increase in intracellular [Ca^{2+}] that activates a Ca-sensitive K conductance (gK_{Ca}); (3) activation of an electrogenic ionic pump due to changes in distribution of ions across the cell membrane during the previous depolarization; and (4) activation of voltage-dependent inhibitory mechanisms by the previous depolarization alone.

Where they have been extensively investigated, direct inhibitory responses to ACh have been associated largely with muscarinic receptors (e.g., see Krnjević, 1975; McCormick and Prince, 1986a, b). Therefore, a direct mediation of the inhibitory response by nicotinic receptors in the MHb would be highly unusual. Rather, our data suggest that the inhibitory response is an indirect consequence of the preceding ACh-induced depolarization. Indeed, applications of another excitatory agent, Glu, or direct depolarization alone was also associated with postexcitatory periods of inhibition (Figs. 1*A*, 4*C*). In other regions of the nervous system, trains of action potentials are often associated with an AHP (Hotson and Prince, 1980; Morita et al., 1982; Madison and Nicoll, 1984; McCormick et al., 1985) that appears to be due in large part to activation of specialized K conductances by increases in intracellular [Ca^{2+}] during the preceding depolarization. Glutamate-induced depolarizations of hippocampal pyramidal cells may also cause activation of a Ca-sensitive K current (Nicoll and Alger, 1981). MHb neurons respond to direct depolarization with an unusually large AHP (see Fig. 4). The reversal potential of this AHP is consistent with the presumed equilibrium potential for K-mediated slow hyperpolarizations in other thalamic neurons (McCormick and Prince, 1986a), although its Ca^{2+} dependency is not yet known. The presence of this large AHP following even a single action potential (Fig. 4, *A, B*) raises the possibility that the inhibition which follows ACh-induced excitation may merely be a prolonged response of the same type.

The most parsimonious explanation for our data is that the ACh-induced hyperpolarization is due to activation of some hyperpolarizing current. One possibility, therefore, is that the inhibitory response may in large part be due to a K conductance activated by Ca entry through the nicotinic channels (Dwyer et al., 1980) opened by ACh. If one takes into account the increase in $[K]_o$ during the ACh-induced inhibitory responses (5–8 mM; Fig. 8), then a reversal potential in the range of −75 to −90 mV is exactly what would be expected if the hyperpolarization were due predominately to activation of a K conductance. However, we were unable to block the inhibitory phase of ACh responses by bathing the slices in 0.0 Ca^{2+} and 5 mM Mn^{2+}, a procedure that should greatly reduce Ca entry into depolarized neurons and therefore reduce Ca-activated K currents (e.g., Hotson and Prince, 1980; Madison and Nicoll, 1984). Although not conclusive, these data suggest that the ACh-induced inhibition is mediated by an increase in gK other than that associated with entry of Ca^{2+} into the MHb cells.

Extensive exposure (over minutes) of neurons in the peripheral ganglia to cholinergic agonists causes a postexcitation inhibition. This inhibition is due to activation of electrogenic ionic pumps (Brown et al., 1972; Volle, 1980). Similarly, large applications of Glu to hippocampal pyramidal cells also result in activation of an electrogenic ion pump (Thompson and Prince, 1986). These postexcitatory hyperpolarizations, in contrast to those reported here, are associated with little or no increase in input conductance. Our limited data would argue against the major involvement of such ionic pumps in the ACh-induced inhibition of MHb neurons. However, it is entirely possible that all of the mechanisms mentioned above are involved to varying degrees (e.g., see Baylor and Nicolls, 1969), with the relative contribution of each perhaps depending upon the length of exposure to ACh. The neural mechanisms underlying this hyperpolarizing response will require further study.

Although nicotine is one of the drugs most widely used by modern man, the mechanisms by which it produces effects on the CNS are largely unknown. To date, only a few subcortical

regions of the CNS are known to contain neurons that have rapid nicotinic excitatory responses. These include the MHb (this study), interpeduncular nucleus (Brown et al., 1983; Takagi, 1984), spinal cord (Curtis and Ryall, 1966), and perhaps some regions of the thalamus (Phillis, 1971), brain stem (Bradley and Dray, 1972), and hypothalamus (Cobbett et al., 1986). Nicotinic receptors or receptors having mixed nicotinic–muscarinic properties have also been implicated in the regulation of synaptic transmission in the hippocampus and interpeduncular nucleus (Rovira et al., 1983; Brown et al., 1984).

Given the prevalence of nicotinic receptors in the MHb and interpeduncular nuclei and their known connections with the forebrain limbic system, as well as their possible involvement in many different complex behaviors, it is reasonable to suggest that some of the central actions of nicotine may be mediated through increased activation of these nuclei.

References

Baylor, D. A., and J. G. Nicolls (1969) After-effects of nerve impulses on signalling in the central nervous system of the leech. J. Physiol. (Lond.) *203:* 571–589.

Boulter, J., K. Evans, D. Goldman, G. Martin, D. Treco, S. Heinemann, and J. Patrick (1986) Isolation of a cDNA clone coding for a possible neural nicotinic acetylcholine receptor α-subunit. Nature *319:* 368–374.

Bradley, P. B., and A. Dray (1972) Short latency excitation of brain stem neurones in the rat by acetylcholine. Br. J. Pharmacol. *45:* 372–374.

Brown, D. A. (1980) Locus and mechanism of action of ganglion-blocking agents. In *Pharmacology of Ganglionic Transmission,* D. A. Kharkevich, ed., *Handbook of Experimental Pharmacology 53:* 185–236.

Brown, D. A., J. V. Halliwell, and C. N. Scholfield (1971) Uptake of nicotine and extracellular space markers by isolated rat ganglia in relation to receptor activation. Br. J. Pharmacol. *42:* 100–113.

Brown, D. A., M. J. Brownstein, and C. N. Scholfield (1972) Origin of the after-hyperpolarization that follows removal of depolarizing agents from the isolated cervical ganglion of rat. Br. J. Pharmacol. *44:* 651–671.

Brown, D. A., R. J. Docherty, and J. V. Halliwell (1983) Chemical transmission in the rat interpeduncular nucleus *in vitro.* J. Physiol. (Lond.) *341:* 655–670.

Brown, D. A., R. J. Docherty, and J. V. Halliwell (1984) The action of cholinomimetic substances on impulse conduction in the habenulointerpeduncular pathway of the rat *in vitro.* J. Physiol. (Lond.) *353:* 101–109.

Chen, G., R. Portman, and A. Wickel (1951) Pharmacology of 1,1-dimethyl-4-phenylpiperazinium iodide, a ganglion stimulating agent. J. Pharmacol. Exp. Ther. *103:* 330–336.

Cobbett, P., W. T. Mason, and D. A. Poulain (1986) Intracellular analysis of control of supraoptic neurone (SON) activity in vitro by acetylcholine (ACh). J. Physiol. (Lond.) *371:* 216P.

Clarke, P. B. S., C. B. Pert, and A. Pert. (1984) Autoradiographic distribution of nicotine receptors in rat brain. Brain Res. *323:* 390–395.

Clarke, P. B. S., R. D. Schwartz, S. M. Paul, C. B. Pert, and A. Pert (1985) Nicotine binding in rat brain: Autoradiographic comparison of [^{3}H] acetylcholine, [^{3}H] nicotine, and [^{125}I]-α-bungarotoxin. J. Neurosci. *5:* 1307–1315.

Contestabile, A., and F. Fonnum (1983) Cholinergic and GABAergic forebrain projections to the habenula and nucleus interpeduncularis: Surgical and kainic acid lesions. Brain Res. *275:* 287–297.

Contestabile, A., and L. Villani (1983) The use of kainic acid for tracing neuroanatomical connections in the septohabenulointerpeduncular system of the rat. J. Comp. Neurol. *214:* 459–469.

Curtis, D. R., and R. W. Ryall (1966) The excitation of Renshaw cells by cholinomimetics. Exp. Brain Res. *2:* 49–65.

Dennis, M. J., A. J. Harris, and S. W. Kuffler (1971) Synaptic transmission and its duplication by focally applied acetylcholine in parasympathetic neurons in the heart of the frog. Proc. R. Soc. London [Biol.] *177:* 509–539.

Domesick, V. B. (1976) Projections of the nucleus of the diagonal band of Broca in the rat. Anat. Rec. *184:* 391–392.

Dwyer, T. M., D. J. Adams, and B. Hille (1980) The permeability of the endplate channel to organic cations in frog muscle. J. Gen. Physiol. *75:* 469–492.

Gallagher, J. P., W. H. Griffith, and P. Shinnick-Gallagher (1982) Cholinergic transmission in cat parasympathetic ganglia. J. Physiol. (Lond.) *332:* 473–486.

Ginsborg, B. L. (1967) Ion movements in junctional transmission. Pharmacol. Rev. *19:* 289–316.

Goldman, D., D. Simmons, L. W. Swanson, J. Patrick, and S. Heinemann (1986) Mapping of brain areas expressing RNA homologous to two different acetylcholine receptor α-subunit cDNAs. Proc. Natl. Acad. Sci. USA *83:* 4076–4080.

Gottesfeld, Z., and D. M. Jacobowitz (1978) Cholinergic projection of the diagonal band to the interpeduncular nucleus of the rat brain. Brain Res. *156:* 329–332.

Gottesfeld, Z., and D. M. Jacobowitz (1979) Cholinergic projections from the septal-diagonal band area to the habenular nuclei. Brain Res. *176:* 291–394.

Gyermek, L. (1980) Methods for the examination of ganglion-blocking activity. In *Pharmacology of Ganglionic Transmission,* D. A. Kharkevich, ed., *Handbook of Experimental Pharmacology 53:* 63–121.

Herkenham, M., and W. J. H. Nauta (1977) Afferent connections of the habenular nuclei in the rat. A horseradish peroxidase study, with a note on the fiber-of-passage problem. J. Comp. Neurol. *173:* 123–146.

Herkenham, M., and W. J. H. Nauta (1979) Efferent connections of the habenular nuclei in the rat. J. Comp. Neurol. *187:* 19–48.

Hotson, J. R., and D. A. Prince (1980) A calcium-activated hyperpolarization follows repetitive firing in hippocampal neurons. J. Neurophysiol. *43:* 409–419.

Houser, C. R., G. D. Crawford, R. P. Barber, P. M. Salvaterra, and J. E. Vaughn (1983) Organization and morphological characteristics of cholinergic neurons: An immunocytochemical study with a monoclonal antibody to choline acetyltransferase. Brain Res. *266:* 97–119.

Iwahori, N. (1977) A golgi study on the habenular nucleus of the cat. J. Comp. Neurol. *171:* 319–344.

Jahnsen, H., and R. Llinás (1984) Electrophysiological properties of guinea pig thalamic neurones: An in vitro study. J. Physiol. (Lond.) *349:* 205–226.

Kataoka, K., Y. Nakamura, and R. Hassler (1973) Habenulo-interpeduncular tract: A possible cholinergic neuron in rat brain. Brain Res. *62:* 264–267.

Kataoka, K., M. Sorimachi, S. Okuno, and N. Mizuno (1977) Cholinergic and GABAergic fibers in the stria medularis of the rabbit. Brain Res. Bull. *2:* 461–464.

Keller, F., K. Rimvall, and P. G. Waser (1984) Slice cultures confirm the presence of cholinergic neurons in the rat habenula. Neurosci. Lett. *52:* 299–304.

Krnjevic, K. (1975) Chemical nature of synaptic transmission in vertebrates. Physiol. Rev. *54:* 418–540.

Kuhar, M. J., R. N. DeHaven, H. I. Yamamura, H. Rommel-Spacher, and J. R. Simon (1975) Further evidence for cholinergic habenulo-interpeduncular neurons: Pharmacologic and functional characteristics. Brain Res. *97:* 265–275.

London, E. D., S. B. Waller, and J. K. Wamsley (1985) Autoradiographic localization of [^{3}H] nicotine binding sites in the rat brain. Neurosci. Lett. *53:* 179–184.

Madison, D. V., and R. A. Nicoll (1984) Control of repetitive discharge of rat CA1 pyramidal neurones *in vitro.* J. Physiol. (Lond.) *354:* 319–331.

Martin, B. R., and M. D. Aceto (1981) Nicotine binding sites and their localization in the central nervous system. Neurosci. Biobehav. Rev. *5:* 473–478.

McCormick, D. A., and D. A. Prince (1985) Two types of muscarinic response to acetylcholine in mammalian cortical neurons. Proc. Natl. Acad. Sci. USA *82:* 6344–6348.

McCormick, D. A., and D. A. Prince (1986a) Acetylcholine induces burst firing in thalamic reticular neurones by activating a potassium conductance. Nature *319:* 402–405.

McCormick, D. A., and D. A. Prince (1986b) Mechanisms of action

of acetylcholine in the guinea pig cerebral cortex, *in vitro*. J. Physiol. (Lond.) *375:* 169–194.

McCormick, D. A., B. W. Connors, J. W. Lighthall, and D. A. Prince (1985) Comparative electrophysiology of pyramidal and sparsely spiny stellate neurons of the neocortex. J. Neurophysiol. *54:* 782–806.

Morita, K., North, R. A., and T. Tokimasa (1982) The calcium-activated potassium conductance in guinea-pig myenteric neurones. J. Physiol. (Lond.) *329:* 341–354.

Nicoll, R. A., and B. E. Alger (1981) Synaptic excitation may activate a calcium dependent potassium conductance in hippocampal pyramidal cells. Science *212:* 957–959.

Oehme, M., and W. Simon (1976) Microelectrode for potassium ions based on a neutral carrier and comparison of its characteristics with a cation exchange sensor. Anal. Chim. Acta *86:* 21–25.

Paton, W. D. M., and E. J. Zaimis (1951) Paralysis of autonomic ganglia by methonium salts. Br. J. Pharmacol. *6:* 155–168.

Phillis, J. W. (1971) The pharmacology of thalamic and geniculate neurons. Int. Rev. Neurobiol. *14:* 1–48.

Rainbow, T. C., R. D. Schwartz, B. Parsons, and K. J. Kellar (1984) Quantitative autoradiography of nicotinic [^{3}H]·acetylcholine binding sites in rat brain. Neurosci. Lett. *50:* 193–196.

Rotter, A., N. J. M. Birdsall, A. S. V. Burgen, P. M. Field, E. C. Hulme, and G. Aisman (1979) Muscarinic receptors in the central nervous system of the rat. I. Technique for autoradiographic localization of the binding of [^{3}H] propylbenzilylcholine mustard and its distribution in forebrain. Brain Res. Rev. *1:* 141–165.

Rovira, C., Y. Ben-Ari, E. Cherubuni, K. Krnjević, and N. Ropert (1983) Pharmacology of the dendritic action of acetylcholine and further observations on the somatic disinhibition in the rat hippocampus in situ. Neuroscience *8:* 97–106.

Takagi, M. (1984) Actions of cholinergic drugs on cells in the interpeduncular nucleus. Exp. Neurol. *84:* 358–363.

Takeuchi, A., and N. Takeuchi (1960) On the permeability of endplate membrane during the action of transmitter. J. Physiol. (Lond.) *154:* 52–67.

Thompson, S. M., and D. A. Prince (1986) Activation of the electrogenic sodium pump in hippocampal CA1 neurons following glutamate-induced depolarization. J. Neurophysiol. *56:* 507–522.

Tokunaga, A., and K. Otani (1978) Fine structure of the medial habenular nucleus in the rat. Brain Res. *150:* 600–606.

Villani, L., Constestabile, A., and F. Fonnum (1983) Autoradiographic labeling of the cholinergic habenulo-interpeduncular projection. Neurosci. Lett. *42:* 261–266.

Vincent, S. R., W. A. Staines, E. G. McGeer, and H. C. Fibiger (1980) Transmitters contained in the efferents of the habenula. Brain Res. *195:* 479–484.

Volle, R. L. (1980) Nicotinic ganglion-stimulating agents. In *Pharmacology of Ganglionic Transmission,* D. A. Kharkevich, ed., *Handbook of Experimental Pharmacology, 53:* 281–312.

Wilcox, K. S., M. J. Gutnick, and G. R. Christoph (1985) Burst generation in lateral habenular neurons recorded in vitro. Soc. Neurosci. Abstr. *11:* 509.

Woolf, N. J., and L. L. Butcher (1985) Cholinergic systems in the rat brain: II. Projections to the interpeduncular nucleus. Brain Res. Bull. *14:* 63–83.

Woolf, N. J., and L. L. Butcher (1986) Cholinergic systems in the rat brain: III. Projections from the pontomesencephalic tegmentum to the thalamus, tectum, basal ganglia, and basal forebrain. Brain Res. Bull. *16:* 603–637.